Chapter 9
Optimization in Brain? – Modeling Human Behavior and Brain Activation Patterns with Queuing Network and Reinforcement Learning Algorithms

Changxu Wu, Marc Berman, and Yili Liu

Abstract Here we present a novel approach to model brain and behavioral phenomena of multitask performance, which integrates queuing networks with reinforcement learning algorithms. Using the queuing network as the static platform of brain structure and reinforcement learning as the dynamic algorithm to quantify the learning process, this model successfully accounts for several behavioral phenomena related to the learning process of transcription typing and the psychological refractory period (PRP). This model also proposes brain changes that may accompany the typing and PRP practice effects that could be tested empirically with neuroimaging. All of the modeled phenomena emerged as outcomes of the natural operations of the human information processing queuing network.

9.1 Introduction

Elucidating the psychological and physiological processes that mediate cognitive and behavioral performance has been an important topic for a long period of time. This topic for many years was studied exclusively with behavioral techniques, and models of behavioral performance had to be inferred exclusively from behavioral data [13, 45]. Current researchers are now endowed with two addi-

Changxu Wu
Department of Industrial and Systems Engineering, State University of New York (SUNY), Buffalo, NY, USA, e-mail: Changxu@buffalo.edu

Marc Berman
Department of Psychology Department of Industrial and Operations Engineering, University of Michigan, Ann Arbor, MI, USA

Yili Liu
Department of Industrial and Operations Engineering, University of Michigan, Ann Arbor, MI, USA

W. Chaovalitwongse et al. (eds.), *Computational Neuroscience*,
Springer Optimization and Its Applications 38, DOI 10.1007/978-0-387-88630-5_9,

tional techniques to understand and to explain human behavioral performance: neuroimaging and computational modeling. With neuroimaging techniques, such as functional magnetic resonance imaging (fMRI [8]), positron emission tomography (PET [9]), and event-related potentials (ERP [29]), researchers can uncover the neural substrates that mediate behavioral performance. These neuroimaging techniques not only allow researchers to localize where cognitive processes reside in the brain, but also allow researchers to uncover commonalities and dissimilarities between cognitive tasks, discover individual differences, and test psychological theories and models in ways that behavioral techniques alone could not uncover [3].

Computational modeling has also been a powerful technique to simulate and compose models for how behavior is mediated. Computational models can be classified into a number of categories, including, e.g., connectionist [19, 30, 39], symbolic [24, 31], and hybrid [4, 27, 58, 50, 47, 52, 54, 53, 55, 51, 59, 57, 56, 60, 61, 62]. With these computational models, researchers are able to validate, test, and update psychological theories in ways that behavioral testing alone could not do easily.

Here we utilize computational modeling to account for changes in performance both behaviorally and neurally due to practice and learning in the context of transcription typing and the psychological refractory period (PRP; the slowing of a secondary task when it is initiated during the response of a primary task). This novel model unifies many disparate findings together into a single model without needing to make many changes to model parameters.

We chose to model the practice and learning effects in transcription typing and PRP due to the following reasons. First, transcription typing involves intricate and complex interactions of perceptual, cognitive, and motoric processes, and modeling its learning processes can help us understand the underlining quantitative mechanisms in complex motor skill acquisition. Second, there exist brain imaging data on typing and typing related behavior [17, 23] that could be modeled. In addition, human behavioral performance data, such as typing speed and typing variability, have been obtained via several experimental studies (please see the review of Salthouse [43]).

We modeled the learning effect in PRP for similar reasons. First, PRP is the simplest and one of the most basic paradigms to study multitask performance and has been used extensively as a paradigm to study multitask performance. The PRP effect has been applied in many real-world settings such as driving [25] and has been used as a measure of dual-task competency [5, 11]. Therefore, modeling the learning effects in PRP may allow us to account for the basic mechanisms in the acquisition of multitasking skills. Second, an experimental study has been conducted to study the learning effect in PRP [48], which provides important human performance data for modeling. For these reasons we found transcription typing and PRP tasks good candidates to model skill learning behavior.

9.2 Modeling Behavioral and Brain Imaging Phenomena in Transcription Typing with Queuing Networks and Reinforcement Learning Algorithms

9.2.1 Behavioral Phenomena

Salthouse [42] reviewed the major behavioral empirical results of transcription typing and summarized 29 phenomena in this area. John [22] summarized two additional behavioral phenomena found by Gentner [16] and [43]. These 31 behavioral phenomena include 12 basic phenomena, 5 error phenomena, 6 phenomena in typing units, and 8 skill learning phenomena in transcription typing. We have developed a queuing network model that successfully modeled 32 behavioral phenomena in transcription typing including 3 newly discovered eye movement phenomena and 29 of these 31 behavioral phenomena, with the exceptions being 2 phenomena related to reading and comprehension, whose modeling requires significant extensions of our model to include production systems and is a current topic of our ongoing research [47]. In this chapter we focus on modeling the learning aspects of the behavioral phenomena and brain imaging phenomena.

The first typing phenomenon that we modeled was changes in interkey response time of transcription typing, which decreases accordingly to the power law of practice [16]. For example, typing speeds of an unskilled typist (about 30 words per minute [21]) can be improved to that of a skilled typist (about 68 words per minute [42]).

The second phenomenon involved the variability of interkey intervals which decreases with the increased skill of the typist. In addition, the interquartile range of interkey intervals correlates significantly with typist's net interkey intervals ($p < 0.05$ [41]). The third behavioral phenomenon that we modeled that we will describe in this chapter was modeling the rate of repetitive tapping, which is greater among more skilled typists and the correlation between repetitive tapping speed and net typing speed is reliable ($p < 0.05$, [41]).

AQ1

9.2.2 Brain Imaging Phenomena

Recently, brain imaging studies (fMRI and PET) have discovered two phenomena related to transcription typing. First, it has been found that at the beginning stages of learning a visuomotor control task, including transcription typing, the dorsal lateral prefrontal cortex (DLPFC), the basal ganglia, and the pre-SMA are highly activated [31, 40]. After practice, activation of the DLPFC disappears and strong activation is observed in the supplementary motor area (SMA), the basal ganglia, and the primary motor cortex (M1) in addition to slight activation in the somatosensory cortex (S1) [17].

Second, in the well-learned stages of typing (skilled typist in [17]), when stimuli to be typed are repetitive letters (e.g., AAA...), M1 is strongly activated, however, when stimuli to be typed are multiletter sentences (e.g., JACK AND...), M1 is strongly activated, but there is more robust activation in the SMA, the basal ganglia, and S1.

9.2.3 A Queuing Network Model with Reinforcement Learning Algorithms

9.2.3.1 The Static Portion of the Queuing Network Model

Queuing network is a mathematical discipline that is used to simulate and model a wide array of phenomena and systems including manufacturing and computer network performance. A queuing network is a network of servers that provide services to customers that wait in queues before they are serviced. Queuing networks tend to be quite flexible and can allow two or more servers to act in serial, in parallel, or in any network configuration [26, 27]. Computational models based on queuing networks have successfully integrated a large number of mathematical models of response time [26] and multitask performance [27]. A queuing network modeling architecture is called the queuing network. Model human processor (QN-MHP) has been developed and used to generate behavior in real time [28], including simple and choice reaction time [14] and driver performance [44]. The model in this chapter extends QN-MHP by integrating reinforcement learning algorithms and strengthening its long-term memory and nine motor subnetwork servers. In addition, the queuing network approach has also been used to quantify changes in brain activation for different participant populations [4].

The brain, which is an enormously complex network of interconnected systems and subsystems, acts in concert with one another to produce behavior. This idea is supported by evidence from pathway tracing studies in nonhuman primates, which revealed widely distributed networks of interconnected cortical areas, providing an anatomical substrate for large-scale parallel processing in the cerebral cortex [6]. It seems, then, that brain areas do not act in isolation from another and instead may form complex neural networks that are the basis of behavior and thought.

In addition to the widely distributed nature of the brain, each brain area may also have some level of functional specialization [9] and thus each major brain area may have certain information processing capacities and certain processing time parameters (see Table 9.1). Here we assume that the interconnections between major brain areas form a queuing network with each major brain area composing a queuing network server and that information processed at each server is a queuing network entity. In addition, neuron pathways that connect major brain areas serve as routes between our queuing network servers (see Fig. 9.1 for transcription typing routing and Fig. 3.1 a for PRP routing. Note that both networks have the same servers and overall network configurations). Therefore, it is assumed that the major brain areas form a queuing network with brain areas as the servers, information processed as

entities, and neuron pathways as routes (see Fig. 9.1). Within this general information processing structure, the major brain areas activated in the transcription typing task 10 were identified by the following fMRI and PET studies ([23, 40, 17], see Fig. 9.1).

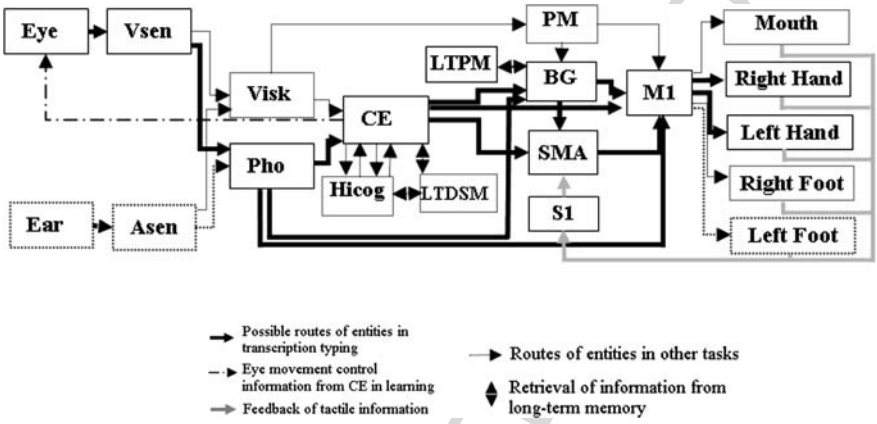

Fig. 9.1: The general structure of the queuing network model (QN-MHP) with routes and servers involved in transcription typing tasks highlighted (server names, brain structures, and processing logic and time are shown in Table 9.1).

([10, 27]. Processing logic and time is based on [38, 14, 37]) If we consider the network for transcription typing, as shown in Fig. 9.1, upon completing service at the Pho server, entities have numerous possible routes to follow to traverse the network: (1) At the Pho server, the entities can choose one of the three routes to depart the Pho server to the CE, BG, or M1 servers. (2) At the CE server, entities can choose to move to the BG, SMA, or M1. (3) At the BG server, entities can move to the SMA or M1 servers. Therefore, there are a total of $3 \times 3 \times 2 = 18$ possible routes for the entities to be processed in the network in transcription typing. An important question is, therefore, how the entities choose among these routes that activate (utilize) different brain areas (servers) in different learning stages or when processing different stimuli at well-learned stages? This question can be answered by the dynamic part of the model.

AQ2

9.2.3.2 The Dynamic Portion of the Queuing Network Model: Self-Organization of the Queuing Network with Reinforcement Learning Algorithms

Ungerleider et al. [44] found evidence for the reorganization of brain areas with practice, which indicates that individual brain areas may change their information processing speeds in learning. Moreover, some brain areas may have error detection

AQ3

Table 9.1: Server name, major function, and brain structure

Server	Brain structure	Major function (Processing logic)
Eye	Eye, LGN, SC, Visual pathway	Visual sampling and signal transmission
VSen	Distributed parallel area, superior frontal sulcus, dorsal and ventral system	Visual sensory memory and perception
Pho	Left posterior parietal cortex, inferior parietal lobe	Phonological loop to store auditoria and textual information
CE	Dorsal lateral prefrontal cortex and ACC	Mental process and response inhibition and selection
BG	Basal ganglia	Motor program retrieval
LTPM	Striatal and cerebellar systems	Long-term procedural knowledge storage
SMA	Supplementary motor area and pre-SMA	Motor program assembly, error detection, and bimanual coordination
M1	Primary motor cortex	Addressing spinal motorneourons
S1	Somatosensory cortex	Sending the sensory information to other areas
Hand	–	Execution of motor movement

functions but others may not (see Table 9.1). Because the routes of the queuing network are composed of different brain areas (servers), different routes chosen by the entities may lead to different information processing speeds or errors. If the entities try to maximize response time performance, they may choose an optimal route that maximizes speed, but may not minimize error. Some routes, however, may maximize both performance measures. Therefore, in different situations, different routes may be chosen by the entities which activate different brain areas (servers). This ability to have different routes becoming active forms the dynamic, self-organization aspect of the queuing network. Consequently, there are two levels of learning within the queuing network: (1) learning processes at the individual server level and (2) self-organization or routes of the queuing network that change depending on the stages of learning or the type of stimuli presented.

Learning Processes of the Individual Servers

In the motor learning process, the basal ganglia, striatal, and cerebellar systems (BG and LTPM servers) play a major role in procedural knowledge acquisition [2]. Therefore, the current model focuses on the BG and the LTPM servers in quantifying the learning processes of individual servers. It is assumed that the time for the BG server to retrieve a motor program from the LTPM decreases exponentially as a function of the number of practice trials (see Equation 9.1). Because the exponential function fits learning processes of memory search, motor learning, visual search,

mathematic operation tasks better than the power law [19] and has been applied in modeling long-term memory retrieval [1] we used it to model our individual server learning processes:

$$1/\mu_{\mathrm{BG}} = A_{\mathrm{BG}} + B_{\mathrm{BG}} \exp -\alpha_{\mathrm{BG}} N_{\mathrm{BG}}, \tag{9.1}$$

$1/\mu_{\mathrm{BG}}$: motor program retrieving time; A_{BG}: the minimal of processing time of BG server after practice (314 ms, [35]); B_{BG}: the change of expected value of processing time from the beginning to the end of practice ($2 \times 314 = 628$ ms, assumed). α_{BG}: the learning rate of server BG (0.00142, [18]); N_{BG}: number of digraphs (letter pairs excluding the space key) processed by server BG, which is implemented as a matrix of diagraph frequency recorded in LTPM server.

Self-Organization of the Queuing Network

If the entities traversing the network try to maximize their information processing speed and minimize error, it is appropriate to apply reinforcement learning algorithms to quantify this dynamic process. Reinforcement learning is a computational approach able to quantify how an agent tries to maximize the total amount of reward it receives in interacting with a complex, uncertain environment [46]. Reinforcement learning has also been applied in modeling motor learning in neuroscience [33] and, therefore, may be appropriately applied to model brain network organization. To integrate the reinforcement learning algorithms with the queuing network approach, it is necessary to define the state, transitions, and reward values of reinforcement learning with the concepts of queuing networks. Below are the definitions:

1. *State:* the status that an entity is in server i.
2. *Transition:* An entity routed from server i to j.
3. *Time-saving reward (r'_t):* $r'_t = (1/w_q) + \mu_{j,t}$ (2)
   w_q: time the entity spent waiting in the queuing of the server; $\mu_{j,t}$: processing speed of the entity at that server.
4. *Error-saving reward (r''_t):* $r''_t = 1/(N\mathrm{error}_{j,t} + 1)$ (3)

$N\mathrm{error}_{j,t}$: number of action errors of the previous entities made in the next server j at tth transition. Q online learning algorithms in reinforcement learning are used to quantify the processes that are used by entities to choose different routes based on rewards of different routes.

1. Q **online learning algorithm of time-saving reward**

$$Q_T^{t+1} Q_T^t(i,j) + \varepsilon\{r'_t + \gamma \max_k [Q_T^t(j,k)] - Q_T^t(i,j)\}, \tag{9.2}$$

   ε: learning rate of Q online learning ($0 < \varepsilon < 1$, $\varepsilon = 0.99$);
   γ: discount parameter of routing to next server ($0 < \gamma < 1, \gamma = 0.3$);
   $Q_T^t + 1(i,j)$: online Q value if entity routes from server i to server j in $t+1$th transition based on time-saving reward;

$\max_k[Q_T^t(j,k)]$: maximum Q value routing from server j to the next k server(s) ($k \geq 1$).
Equation (9.2) updates a Q value of a backup choice of routes ($Q_T^t(i,j)$) based on the Q value which maximizes over all those routes possible in the next state ($\max_k[QtT(j,k)]$). In each transition, entities will choose the next server according to the updated $Q_T^t(i,j)$.

2. Q **online learning algorithm of error-saving reward**

$$Q_E^{t+1}Q_E^t(i,j) + \varepsilon\{r_t'' + \gamma \max_k[Q_E^t(j,k)] - Q_E^t(i,j)\}. \tag{9.3}$$

3. **Trade-off of the two Q values**

The choice of routes is determined by the trade-off between the two Q values. Currently, it is assumed that $Q_E^{t+1}(i,j)$ of error-saving reward has the higher priority than the $Q_T^{t+1}(i,j)$ of time-saving reward: if $Q_E^{t+1}(i,j) > Q_E^{t+1}(i,k)$, the entity will choose the next server j whatever the value of $Q_T^{t+1}(i,j)$; if $Q_E^{t+1}(i,j) = Q_E^{t+1}(i,k)$, entity will choose the next server with greater Q_T^{t+1}; if $Q_E^{t+1}(i,j) = Q_E^{t+1}(i,k)$ and $Q_T^{t+1}(i,j) = Q_T^{t+1}(i,k)$, entity will choose next server randomly. With these equations, we were able to successfully integrate queuing networks with reinforcement learning algorithms.

9.2.4 Model Predictions of three Skill Learning Phenomena and two Brain Imaging Phenomena

The three skill learning phenomena and the two brain imaging phenomena of transcription typing described earlier in this chapter can be predicted by the queuing network model with reinforcement learning.

9.2.4.1 Predictions of the three Skill Learning Phenomena

We assume that the processing times of the CE, BG, and SMA servers follow the exponential distribution (see Table 9.1 and Fig. 9.1) and are independent from one another. Therefore, if $Y_1 \cdots Y_k$ are k independent exponential random variables representing the processing times of the servers in our network, their sum X follows an Erlang distribution. Based on features of Erlang distributions, we have

$$X = \sum_{i=1}^{k} Y_i, \tag{9.4}$$

$$E[X] = E\left[\sum_{i=1}^{k} Y_i\right] = \sum_{i=1}^{k} E[Y_i] = k\frac{1}{\lambda}, \tag{9.5}$$

$$\mathrm{Var}[X] = \mathrm{Var}\left[\sum_{i=1}^{k} Y_i\right] = \sum_{i=1}^{k} \mathrm{Var}[Y_i] = k\frac{1}{\lambda^2}. \tag{9.6}$$

These mathematical results can be used to predict the skill learning phenomena, together with the prediction described below that entities may learn to skip certain server(s). First, because $E[X] = k(1/\lambda)$, if $k' < k$, then it follows that $E[X'] < E[X]$. This may be one of the reasons that the skipping of server(s) can explain a reduction in interkey time in typing normal text (the first skill learning phenomenon in this chapter) and repetitive letters (the third skill learning phenomenon). Second, skipping some of the servers will decrease the variance of the Erlang distribution because if $k' < k$, then $\mathrm{Var}[X'] < \mathrm{Var}[X]$. This is one possible reason why skipping over server(s) can account for the reduction in the variability of interkey time in the learning process (the second skill learning phenomenon).

9.2.4.2 Predictions of the First Brain Imaging Phenomenon

At the Pho server during the initial stages of learning, entities can go through the CE server for eye movement control to locate the specific position of a target key on the keyboard ([12], see Fig. 9.1) and for response selection and inhibition. Entities can also traverse the route from Pho to BG, but it takes longer than going through the CE because the BG may not work effectively in retrieving the motor program from LTPM [2] and its Q value of time-saving reward is smaller than that of CE. Entities can also choose the route from Pho→ M1 directly. However, the occurrence of typing errors will decrease the Q value of error-saving reward from 18 Pho→M1. As the number of practice trials increases, the route Pho→BG is selected by the majority of the entities because the functions of CE are gradually replaced by the BG with less process time based on parallel cortico-basal ganglia mechanisms [33].

Second, at the CE server, entities can traverse one of the routes from CE to BG, SMA, or M1. If entities select the first route, the correct motor program will be retrieved without decreasing the $Q_E^{t+1}(i,j)$ value. If the second or the third route is chosen, its $Q_E^{t+1}(i,j)$ value will decrease because no correct motor program is retrieved.

The third prediction involves the BG server. Since stimuli keep changing in typing multidigit sentences, entities can go from the BG directly to M1 skipping SMA whose function is motor program assembling [36]. However, ensuring movement accuracy for error detection [17] will decrease $Q_E^{t+1}(i,j)$ in route BG…M1. In sum, at the beginning of the learning process, entities will go through Pho→ CE→BG→SMA→M1. After learning, the majority of entity will travel Pho→BG→ SMA→M1.

9.2.4.3 Predictions of the Second Brain Imaging Phenomenon

If stimuli change from repetitive letters to regular words in the same task, the entities will change routes from Pho→M1 to Pho→BG→SMA→M1 because the error-saving reward decreases in route Pho…M1 without the motor program functions of

BG and the sequencing functions of SMA. This is our second prediction of changes in neural processing with learning.

9.2.5 Simulation of the three Skill Learning Phenomena and the two Brain Imaging Phenomena

9.2.5.1 The First and the Second Skill Learning Phenomena

Simulation results showed that the simulated interkey interval in the learning process followed the power law of practice (R square $= 0.8$, $p < 0.001$). The simulated interkey interval also improved from 385 to 180 ms, which was consistent with existing experimental data about performance changes from the unskilled typist (interkey time 400 ms) with estimation error 3.75% (estimation error $= |YX|/X \times 100\%$, Y: simulation result; X: experiment result) to the skilled typist (177 ms interkey time) with estimation error 1.69% (see Fig. 9.1).

As shown in Fig. 9.2, the change of the quartile range (75% quartile–25% quartile) is significantly correlated with the change of the simulated speed ($p < 0.05$), which is consistent with the experimental results of Salthouse [41]. This was one of the phenomena not covered by TYPIST [22].

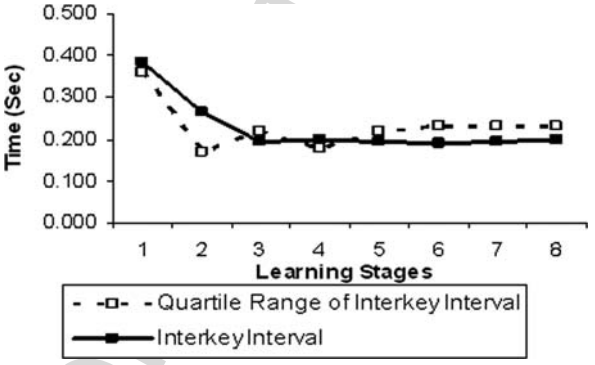

Fig. 9.2: Simulated variability of interkey interval and interkey interval in the learning process. Each stage represents 352,125 keystrokes.

9.2.5.2 The Third Skill Learning Phenomena

The simulated tapping rate (interkey interval in typing repetitive letters) and typing speed of text (interkey interval in typing multidigit sentence) during the learning process were found to be strongly correlated ($p < 0.05$), which is consistent with the experimental results of Salthouse [41] who found the significant correlation between the two variables ($p < 0.01$). Therefore, our model successfully modeled these behavioral phenomena with very high accuracy.

9.2.5.3 The First Brain Imaging Phenomena

As shown in Fig. 9.3, at the beginning of practice, the CE (including DLPFC) and the BG servers are highly utilized, while the SMA server (including pre-SMA) (3%) and M1 and two hand servers (15%) are less utilized. After $352,125 \times 8$ trials of practice, the CE server (DLPFC) decreased its utilization greatly to 0%. Percentage of utilization of SMA server is increased by 47%. M1 and two hand servers and S1 also increased their percentage of utilization during the learning process by 85% and 22%, respectively. These simulation results are consistent with the experimental results in PET and fMRI studies [23, 40, 17] who found similar patterns of increases and decreases in brain activity.

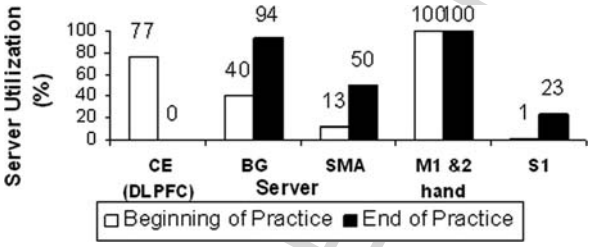

Fig. 9.3: Server utilization at the beginning and end of practice in learning to type multidigit sentence.

9.2.5.4 The Second Brain Imaging Phenomena

After the model finished its learning process, it was able to simulate the second brain imaging phenomenon of the skilled typist in typing different stimuli. The 1,600 letters to be typed by the model changed following this pattern: 1st – 800th letters: repetitive letters; 801st – 1,600 letters: multidigit sentence.

Figure 9.4 shows the percentage of utilization of the major servers in the different stimulus conditions. When the model is typing repetitive letters, mainly M1 and two hand servers are utilized. When the stimuli changed from repetitive letters to multidigit sentences the utilization of SMA, BG, and S1 increased by 49, 90, and

Fig. 9.4: Server utilization when stimuli presented changed in the well-learned transcription typing situation.

22%, respectively. The model demonstrated that fewer entities travel from Pho to M1 directly when the stimuli presented changes from repetitive letters to multidigit sentences. These results are consistent with the fMRI results of [17].

In practice, because our queuing network model was built with a general structure with common brain regions, it can be easily transformed to model other task situations, e.g., PRP [49]. Moreover, the current model can generate behavioral results by the interaction of the queuing network servers without drawing complex scheduling charts. These unique features offer great potential of the model for learning and can easily be used by researchers in cognitive modeling and human factors.

9.3 Modeling the Basic PRP and Practice Effect on PRP with Queuing Networks and Reinforcement Learning Algorithms

PRP (Psychological Refractory Period) is one of the most basic and simple forms of dual-task situations and has been studied extensively in the laboratory for half a century [31]. In the basic PRP paradigm, two stimuli are presented to subjects in rapid succession and each requires a quick response. Typically, responses to the first stimulus (Task 1) are unimpaired, but responses to the second stimulus (Task 2) are slowed by 300 ms or more . In the PRP paradigm of Van Selst et al. [48], task 1 required subjects to discriminate tones into high or low pitches with vocal responses (audio-vocal responses); in task 2 subjects watched visually presented characters and performed a choice reaction time task with manual responses (visual-motor responses). They found that practice dramatically reduced dual-task interference in PRP.

The basic PRP effect has been modeled by several major computational cognitive models based on production rules, notably EPIC [31] and ACT-R/PM [7]. Based on its major assumption that production rules can fire in parallel, EPIC successfully modeled the basic PRP effect by using complex lock and unlock strategies in central processes to solve the time conflicts between perceptual, cognitive, and motor processing [31]. However, neither EPIC nor ACT-R/PM modeled the practice effect on PRP.

Here we modeled PRP effects with the same model that modeled typing phenomena and integrated queuing network theory [26, 27] with reinforcement learning algorithms [46]. Model simulation results were compared with experimental results of both the basic PRP paradigm and the PRP practice effects [48]. All of the simulated human performance data were derived from the natural interactions among servers and entities in the queuing network without setting up lock and unlock strategies or drawing complex scheduling charts.

9.3.1 Modeling the Basic PRP and the Practice Effect on PRP with Queuing Networks

Figure 9.5 shows the queuing network model that was used to model PRP effects. The model architecture is identical to the model that was used to model typing

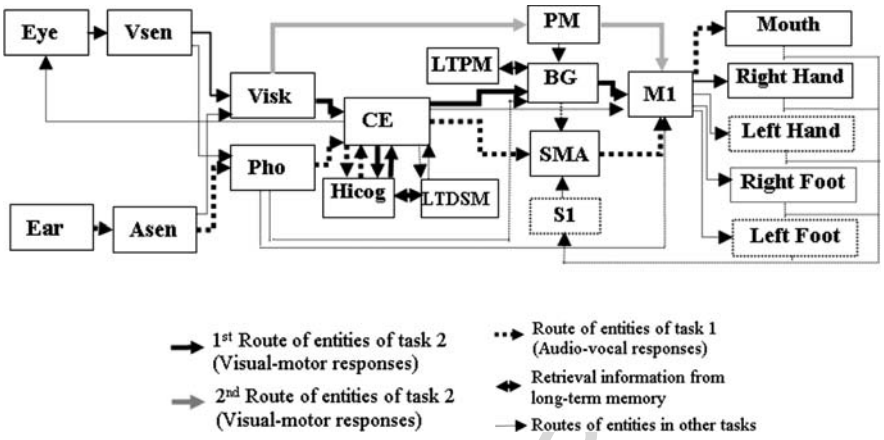

Fig. 9.5: The general structure of the queuing network model (QN-MHP) with servers and routes involved in the PRP task highlighted (server names, brain structures, major functions, and processing time are shown in Table 9.1).

phenomena. However, entities traverse different routes while performing PRP tasks than they traversed when performing typing tasks.

Because the PRP effect prior to or at the beginning of learning (the basic PRP) is a special case of the PRP effect during the learning process, the two phenomena of PRP (basic and learned) are modeled with the same mechanisms in our queuing network model. The experimental tasks and data of Van Selst et al. [48] were used to test the model.

Brain areas (servers) and their routes related to the two PRP tasks in Van Selste's study were identified within the general queuing network structure based on recent neuroscience findings [32, 15, 2], see Fig. 9.5). When exploring Fig. 9.5 entities of task 1 (audio-vocal responses) cannot bypass the Hicog server because the 26 phonological judgment function is mainly mediated by the Hicog server, and thus there is only one possible route for the entities of task 1 (see the dotted thick line in Fig. 9.5) to traverse. However, the function of movement selection in task 2 (visual-motor responses) is located not only in the Hicog server but also in the PM server. Therefore, there are two possible routes for the entities of task 2 starting at Visk server (see the gray and black solid lines in Fig. 9.5).

However, how might the entities of task 2 choose one of the two alternative routes in the network? What is the behavioral impact of this choice on PRP and the practice effect on PRP? These questions can be answered by integrating queuing networks with reinforcement learning algorithms. Before exploring the mechanism with which entities of task 2 select from one of the two routes, it is necessary to understand the learning process of individual brain areas. It was discovered that each individual brain area reorganizes itself during the learning process and increases its processing speed [44]. For example, for the simplest network with two routes (see Fig. 9.6), if servers 2 and 3 change their processing speeds, different routes chosen by an entity (1→3→4 or 1→2→4) will lead to different performance. Without con-

sidering the effect of error, entities will choose the optimal route with the shortest processing time if they want to maximize the reward of performance.

Consequently, to model learning, it is first necessary to quantify the learning process in individual servers. Based on that, the condition under which an entity switches between the two routes shown in Fig. 9.6 can be established and proved by integrating queuing network with reinforcement learning. Finally, this quantitative condition of route switching can be applied to the more complex model of 18 servers with two routes (see Fig. 9.5) to generate the basic PRP and the reduction of PRP during the learning process.

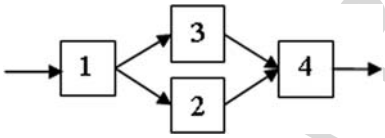

Fig. 9.6: The simplest queuing network with two routes.

9.3.1.1 Learning Process in Individual Servers

Based on the functions of the servers in Table 9.1, the two long-term memory servers (LTDSM and LTPM) play the major roles in learning phonological judgments (task 1) and choice reaction (task 2) [2]. Because the learning effects of long-term memory are represented as speed of retrieval of production rules and motor programs from the two long-term memory servers at the Hicog and the BG servers, it is important to quantify the processing time of the Hicog and the BG servers. In addition, because the premotor cortex (PM) server is activated in learning visuomotor associations [32], changes in the processing speed of the PM server is also to be considered in the learning process of the model.

Because the exponential function fits the learning processes in memory search, motor learning, visual search, and mathematic operation tasks better than the power law [18], it was again applied to model the learning process in the individual servers here

$$1/\mu_i = A_i + B_i \mathrm{Exp}(-\alpha_i N_i), \tag{9.7}$$

μ_i: processing speed of the server i; $(1/\mu_i)$ is its processing time; A_i: the minimal of processing time of server i after intensive practice; B_i: the change of expected value of processing time of server i from the beginning to the end of practice; α_i: learning rate of server i; N_i: number of customers processed by server i.

For the BG server, $1/\mu_{\mathrm{BG}}$: motor program retrieving time; ABBGB: the minimal of processing time of BG server after practice (314 ms, [35]); B_{BG}: the change of expected value of processing time from the beginning to the end of practice ($2 \times 314 = 628$ ms, assumed); α_{BG}: the learning rate of server BG (0.00142, [18]); N_{BG}:

number of entities processed by server BG which is implemented as a matrix of frequency recorded in LTPM server.

For the Hicog and PM servers, to avoid building an ad hoc model and using the result of the experiment to be simulated directly, nine parameters in the Hicog and the PM servers were calculated based on previous studies (see Appendix 1). AQ7

9.3.1.2 Learning Process in the Simplest Queuing Network with two Routes

Based on the learning process of individual servers, the condition under which an entity switches between the two routes in the simplest form of queuing networks with two routes (each capacity equals 1) (from route 1…2…4 to route 1…3…4, see Fig. 9.6) was quantified and proved by the following mathematical deduction.

1. Q **online learning equation [46]**

$$Q^{t+1}(i,j)Q^{t}(i,j)+\varepsilon\{r_t+\gamma\max_k[Q^t(j,k)-Q^t(i,j)], \tag{9.8}$$

where $Q^{t+1}(i,j)$ is the online Q value if entity routes from server i to server j in $t+1$th transition; $\max_k[Q(j,k)]$ represents maximum Q value routing from server j to the next k server(s) ($k \leq 1$); $r_t = \mu_{j,t}$ is the reward and is the processing speed of the server j if entity enters it at tth transition; N_{jt} represents number of entities go to server j at tth transition; ε is the learning rate of Q online learning ($0 < \varepsilon < 1$); γ is the discount parameter of routing to next server ($0 < \gamma < 1$); and p is the probability of entity routes from server 1 to server 3 does not follow the Q online learning rule if $Q(1,3) > Q(1,2)$. For example, if $p = 0.1$, then 10% of entity will go from server 1 to server 2 even though $Q(1,3) > Q(1,2)$.

State is the status that an entity is in server i; transition is defined as an entity routed from server i to j. Equation (9.8) updates a Q value of a backup choice of routes ($Q^{(t+1)}(i,j)$) based on the Q value which maximizes over all those routes possible in the next state ($\max_k[Q(j,k)]$). In each transition, entities will choose the next server according to the updated $Q^t(i,j)$. If $Q(1,3) > Q(1,2)$, more entity will go from server 1 to server 3 rather than go to server 2.

2. **Assumption**
   - ε is a constant which does not change in the current learning process ($0 < \varepsilon < 1$) .
   - Processing speed of server 4 (μ_4) is constant.
3. **Lemma 9.1.** At any transition state t ($t \neq 0$), if $1/\mu_{2,t} < 1/\mu_{3,t}$ then $Q^{t+1}(1,2) > Q^{t+1}(1,3)$
   Proof of Lemma 9.1 (see Appendix 2).
   Based on Lemma 9.1 and Equation (9.7), we got Lemma 9.2:
4. **Lemma 9.2.** At any transition state t ($t \neq 0$), if $A_2 + B_2\text{Exp}(\alpha_2 N_{2t}) < A_3 + B_3\text{Exp}(-\alpha_3 N_{3t})$ then $Q^{t+1}(1,2) > Q^{t+1}(1,3)$.

9.3.2 Predictions of the Basic PRP and the Practice Effect on PRP with the Queuing Network Model

Based on Equation (9.7) and Lemmas 9.1 and 9.2, we can predict the simulation results of the basic PRP effect and the PRP practice effect. For the entities in task 2 (see Fig. 9.5), at the beginning of the practice phrase, because the visual-motor mappings are not established in PM [32], PM takes a longer time to process the entities than the CE and the Hicog servers. Thus, the Q value from Visk to PM ($Q(1,3)$) is lower than the Q value from Visk to CE ($Q(1,2)$). According to Lemma 9.1, the majority of the entities will go to the CE and Hicog server at the beginning of the learning process in dual tasks. Consequently, entities from task 1 also go through the CE and Hicog server thus producing a bottleneck at the Hicog server which produces the basic PRP effect. This bottleneck is similar in theory to that of Pashler [34].

During the learning process, the CE will send entities which increase the processing speed of PM based on the parallel learning mechanisms between the visual loop (including CE) and the motor loop (including PM) ([33], see Table 9.1). Therefore, when the Q value of the 2P and P route of task 2 increases, an increasing number of entities of task 2 will travel on the 2nd route and form an automatic process, which creates two parallel routes that could be traversed in this dual-task situation. However, because the learning rate of PM server (1/16,000) is lower than that of the Hicog server for the entities in task 2 (1/4,000), the majority of the entities will still go through the Hicog server.

9.3.3 Simulation Results

Figure 9.7 shows the simulation results of the basic PRP effect compared to the empirical results (Van Selst et al., 1999). The linear regression function relating the simulation and experimental results 32 is: $Y = 1.057X - 58$ (Y: experiment result;

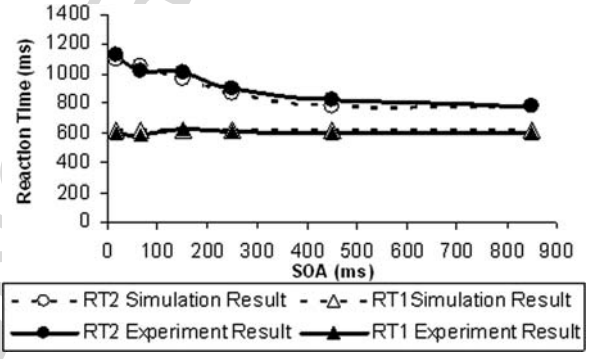

Fig. 9.7: Comparison of simulation and experiment results at the beginning of practice (basic PRP effect).

X: simulated result; R square $= 0.984$, $p < 0.001$;). Therefore, our model fits the data well.

Figure 9.8 compares of simulation and experiment results of the PRP effect at the end of practice (after 7,200 fs trials). The linear regression function relating the simulated results and experiment results is: $Y = 1.03X + 105$ (R square $= 0.891$, $p < 0.001$), therefore, our model accurately captures learning effects related to the PRP effect.

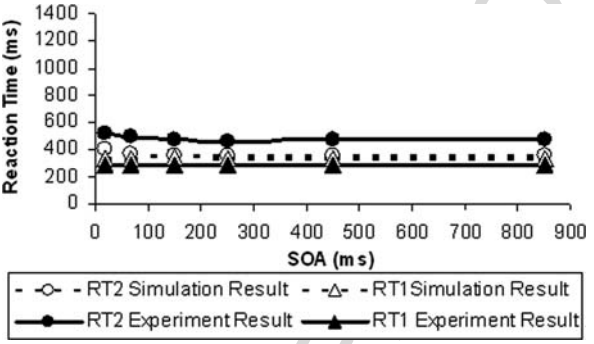

Fig. 9.8: Comparison of the simulation and experiment results at the end of practice.

Lastly, Fig. 9.9 shows the comparison of the simulation and experimental results during the practice process (7,200 trials). The linear regression function relating the simulated results and experiment results is: $Y = 0.965X + 10$ (R square $= 0.781$, $p < 0.001$). Moreover, it was found that the Q value of the second route of task 2 never exceeded that of the first route of task 2 during the practice process as

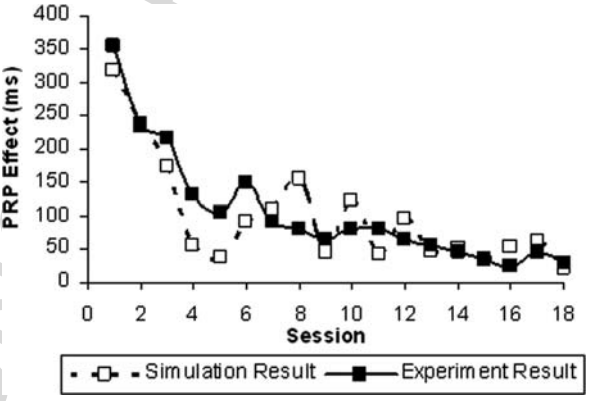

Fig. 9.9: Comparison of simulation and experiment results during the practice process (7,200 trials).

the majority of entities of task second went through the first route rather than the second route. In some ways this is supported by recent neuroimaging work on PRP by [20]. Those authors found little 33 differences in activations/neural networks in the PRP task when performance was assessed at long and short SOAs. Such large activation differences between short and long SOAs would be predicted by active monitoring theories of the PRP effect. However, Jiang et al. [20] contend that their data suggest that the PRP effect reflects passive queuing and not active monitoring. This is yet other evidence supporting the queuing network architecture and structure of our model as we did not find much difference in performance in the Hicog server before and after practice and at short and long SOAs. In addition, routes are chosen passively with Q learning and are not subject to active monitoring processes.

With the formation of an automatic process during learning, two parallel routes were formed in the dual-task situation, which partially eliminated the bottleneck at the Hicog server. The PRP effect is reduced greatly with the decrease in the processing time in both the Hicog and the PM server. However, since the majority of the entities of the two tasks still went through the Hicog server, the effect of the automatic process on PRP reduction does not exceed the effect of the reduction of RT 1 on the PRP effect. This is consistent with the result of Van Selst et al. [48] that the automatic process does grow from weak to strong but only weakly contributes to PRP reduction.

9.4 Discussion

In the previous sections of this chapter, we described the modeling of brain activation patterns as well as the behavioral phenomena in learning of two basic perceptual-motor tasks (transcription typing and PRP). In modeling the phenomena in typing, reinforcement algorithms guided how the entities traversed through different routes before and after learning. The brain areas activated both before and after learning are consistent with neuroimaging findings. In modeling PRP practice effects, we used the same simulation model to quantify the formation of automatic processes (reduction of the visual-motor task 2) during the learning processes in Van Selst et al. [48] study.

There are several questions to be answered by future research utilizing our model. First, neuroscience evidence has shown that many brain areas have overlapping functionality which was not captured by the current model, which assumed discrete brain areas with specific functions. This will increase the difficulty in modeling the cooperation of information processes in the different brain areas. Second, the traveling of entities from one server to another does not necessarily indicate the activation of two brain areas. Brain area activation as uncovered with fMRI studies is based on brain hemodynamics, which is an indirect measure of neural activity and thus has poor temporal resolution. Therefore, using fMRI data to guide modeling of processing times is somewhat tenuous. Therefore, 35 caution should be taken in comparing the simulation results of the model with the results of fMRI studies.

We are currently developing a computational model of the human cognitive system which is able to account for experimental findings in both neuroscience and behavioral science. It is one step further to understanding the quantitative mechanisms of complex cognition and provides an alternative way to connect the brain's function with overt behavioral phenomena. We believe this current model is a firm step in this direction.

Parameters setting at Hicog and PM server

- $A_{\text{Hicog-symbol}}$: minimal value of the processing time of task 2 entity in Hicog server. Since choice reaction time (RT) of four alternatives can be reduced to RT of two alternatives with practice (Mowbray et al., 1959), after intensive practice, RT of eight alternative choices in Van Selst's experiment will reduce to RT of four alternatives without intensive practice. $A_{\text{Hicog-symbol}}$ equals the RT of four alternatives (Hick's Law, intercept:150 ms, slope:170 ms/bit, Schmidt, 1988) minus one average perception cycle (100 ms), two cognitive cycles (2×70 ms), and one motor cycle (70 ms) [10]. Therefore, $A_{\text{Hicog-symbol}} = 150 + 170 \times \text{Log2}(4) - 100 - 2 \times 70 - 70 = 180$ ms.
- $B_{\text{Hicog-symbol}}$: change of processing time of task 2 entity in Hicog server at the beginning and end of practice. At the beginning of the practice in single task 2, RT of the eight alternatives (Hick's Law, intercept:150 ms, slope:170 ms/bit, Schmidt, 1988) is composed of one perception cycle (100 ms), maximum processing time at Hicog ($\text{A}_{\text{Hicog-symbol}} + \text{B}_{\text{Hicog-symbol}}$), and one motor cycle (70 ms) [10]. Therefore, $B_{\text{Hicog-symbol}} = 150 + 170 \times \text{Log2}(8) - 100 - A_{\text{Hicog-symbol}} - 70 = 170$ ms.
- $\alpha_{\text{Hicog-symbol}}, \alpha_{\text{Hicog-tone}}$: learning rate of Hicog server in processing the task 2 and task 1 entities. Based on $\alpha = 0.001$ approximately in Heathcote et al.'s [18] study, learning difficulty increased four times because of the four incompatible alternatives. Thus, $\alpha_{\text{Hicog-symbol}} = \alpha_{\text{Hicog-tone}} = 0.001/4 = 1/4{,}000$.
- $\mathbf{A}_{\text{Hicog-tone}}$: minimal value of the processing time of task 1 entity in central executive. After intensive practice, the discrimination task of the two classes of tones in Van Selst's (1999) experiment can be simplified into a choice reaction time of two alternatives, requiring the minimum value of one cognitive cycle (25 ms) [10].
- $\mathbf{B}_{\text{Hicog-tone}}$: change of processing time of task 1 entity in Hicog at the beginning and end of practice. At the beginning of the single task 1, the reaction time to discriminate the two classes of tone is 642 ms (Flynn, 1943), which is composed of one perception cycle (100 ms), two cognitive cycles (70×2 ms), ($\text{A}_{\text{Hicog-tone}} + \text{B}_{\text{Hicog-tone}}$), and one motor cycle (70 ms). Therefore, $B_{\text{Hicog-tone}} = 642 - 100 - 2 \times 70 - A_{\text{Hicog-tone}} - 70 = 307$ ms.
- $\mathbf{A}_{\text{PM-symbol}}$: minimal value of the processing time of task 2 entity in PM. After intensive practice, RT of the eight alternative choices in Van Selst's experiment will transform to RT of eight most compatible alternatives (RT = 217 ms, Schmidt, 1988) which is composed of one perception cycle and one motor cycle. Therefore, $A_{\text{PM-symbol}} = 217 - 100 - 70 = 47$ ms.

- $\mathbf{B}_{\text{PM-symbol}}$: change of processing time of task 2 entity in PM at the beginning and end of practice. At the beginning of practice in single task 2, RT of eight alternative choice reaction time (Hick's law: 50 ms, slope: 170 ms/bit) is composed of one average perception cycle (100 ms), ($A_{\text{PM-symbol}} + B_{\text{PM-symbol}}$), one motor cycle (70 ms). Thus, $B_{\text{PM-symbol}} = 150 + 170 \times \text{Log2}(8) - 100 - A_{\text{PM-symbol}} - 70 = 443$ ms.
- $\alpha_{\text{PM-symbol}}$: learning rate of PM in processing the task 2 entity. The speed of formation of the automatic process in PM is slower than Hicog because it receives the entities from CE server via the indirect parallel learning mechanism with the four incompatible alternatives [33]. Thus, $\alpha_{\text{PM-symbol}} = (0.001/4)/4 = 1/16{,}000$.

Appendix

Proof of Lemma 9.1 **Lemma 9.1. At any transition state** t ($t \neq 0$)**, if** $1/\mu_{2,t}, t < 1/\mu_{3,t}$**, then** $Q_{t+1}(1,2) > Q_{t+1}(1,3)$

Proof. Using mathematic deduction method

(i) At $t = 0$: $Q^1(1,3) = Q^1(1,2) = Q^1(2,4) = Q^1(3,4) = 0$.

(ii)At $t = 1$: Using the online Q learning formula: $Q^2(1,3) = Q^1(1,3) + \varepsilon[r_t + \gamma Q^1(3,4) - Q^1(1,3)] = \varepsilon\mu_{3,1}$.

Note: because entity routes to only one server (server 4) $\max_b\ Q^t(S_t+1,b) = Q(3,4), Q^2(1,2) = \varepsilon\mu_{2,1}, Q^2(3,4) = \varepsilon\mu_4, Q^2(2,4) = \varepsilon\mu_4$; If $1/\mu_{2,1} < 1/\mu_{3,1}$ then $\varepsilon\mu_{3,1} < \varepsilon\mu_{2,1}$ (given $0 < \varepsilon < 1$), i.e., $Q^2(1,2) > Q^2(1,3)$. Thus, lemma is proved at $t = 1$.

iii According to mathematic deduction method, Lemma 9.1 is correct: i.e., at transition state $t = k$: if $1/\mu_{2,k} < 1/\mu_{3,k}$ then $Q^{k+1}(1,2) > Q^{k+1}(1,3)$. We want to prove at transition state $k+1$, lemma is still correct: i.e., At transition state $t = k+1$:
if $1/\mu_{2,k+1} < 1/\mu_{3,k+1}$, then $Q^{k+2}(1,2) > Q^{k+2}(1,3)$ At $t = k+1$: $Q^{k+2}(1,2) = Q^{k+1}(1,2) + \varepsilon[\mu_{2,k+1} + \gamma\varepsilon\mu_4 - Q^{k+1}(1,2)]$

$$Q^{k+2}(1,3) = Q^{k+1}(1,3) + \varepsilon[\mu_{3,k+1} + \gamma\varepsilon\mu_4 - Q^{k+1}(1,3)], \tag{9.9}$$

$$Q^{k+2}(1,2) - Q^{k+2}(1,3) = \tag{9.10}$$

$$Q^{k+1}(1,2) + \varepsilon[\mu_{2,k+1} + \gamma\varepsilon\mu_4 - Q^{k+1}(1,2)] - Q^{k+1}(1,3) + \varepsilon[\mu_{3,k+1} + \gamma\varepsilon\mu_4 - Q^{k+1}(1,3)] \tag{9.11}$$

$$= (1-\varepsilon)[Q^{k+1}(1,2) - Q^{k+1}(1,3)] + (\varepsilon\mu_{2,k+1} - \varepsilon\mu_{3,k+1}) \tag{9.12}$$

With Equation (9.3) and $0 < \varepsilon < 1$, we have

$$(1-\varepsilon)[Q^{k+1}(1,2) - Q^{k+1}(1,3)] > 0. \tag{9.13}$$

Given $1/\mu_{2,k+1} < 1/\mu_{3,k+1}$ and $0 < \varepsilon < 1$, then $(\varepsilon\mu_{2,k+1} - \varepsilon, \mu_{3,k+1}) > 0$, i.e., $Q^{k+2}(1,3) - Q^{k+2}(1,2) > 0$

Thus, Lemma 9.1 is correct at $t = k+1$. Lemma 9.1 is proved.

References

1. Anderson, J., Lebiere, C. The Atomic Components of Thought. Erlbaum, Mahwah, NJ (1998)
2. Bear, M., Connors, B., Paradiso, M. Neuroscience: Exploring the Brain. Lippincott Williams & Wilkins Publisher, Baltimore, MD (2001)
3. Berman, M., Jonides, J., Nee, D. Studying mind and brain with fMRI. Soc Cogn Affect Neurosci **1**(2), 158–161 (2006)
4. Berman, M., Liu, Y., Wu, C. A 3-node queuing network template of cognitive and neural differences as induced by gray and white matter changes. In: Proceedings of the 8th International Conference on Cognitive Modeling, pp. 175–180. Ann Arbor, MI (2007)
5. Bherer, L., Kramer, A., Peterson, M., Colcombe, S., Erickson, K., Becic, E. Testing the limits of cognitive plasticity in older adults: Application to attentional control. Acta Psychologica **123**(3), 261–278 (2006)
6. Bressler, S. Large-scale cortical networks and cognition. Brain Res Rev **20**, 288–304 (1995)
7. Byrne, M., Anderson, J. Serial modules in parallel: The psychological refractory period and perfect time-sharing. Psychol Rev **108**(4), 847–869 (2001)
8. Cabeza, K. Handbook of Functional Neuroimaging of Cognition, 2nd edn. MIT Press, Cambridge, MA (2006)
9. Cabeza, R., Nyberg, L. Imaging cognition II: An empirical review of 275 PET and fMRI studies. J Cogn Neurosci **12**(1), 1–47 (2000)
10. Card, S., Moran, T., Newell, A.N. Handbook of perception and human performance, chap. The Model Human Processor: An Engineering Model of Human Performance. Wiley, New York (1986)
11. Dell'Acqua, R., Sessa, P., Pashler, H. A neuropsychological assessment of dual-task costs in closed-head injury patients using Cohen's effect size estimation method. Psychol Res-Psychologische Forschung **70**(6), 553–561 (2006)
12. Deseilligny, C., Muri, M. Cortical control of ocular saccades in humans: A model for motricity. In: Neural Control of Space Coding and Action Production, Progress in Brain Research, Vol. 142, pp. 1–19. Elsevier, New York (2003)
13. Donders, F. Attention and Performance 2, chap. Over de snelheid van psychische processen [On the speed of mental processes]. North-Holland, Amsterdam (1969). (Original work published in 1869)
14. Feyen, R., Liu, Y. Modeling task performance using the queuing network model human processor (qnmhp). In: Proceedings of the 4th International Conference on Cognitive Modeling, pp. 73–78 (2001)
15. Fletcher, P., Henson, R. Frontal lobes and human memory – insights from functional neuroimaging. Brain **124**, 849–881 (2001)
16. Gentner, D. The acquisition of typewriting skill. Acta Psychol **54**, 233–248 (1983)
17. Gordon, A., Soechting, J. Use of tactile afferent information in sequential finger movements. Exp Brain Res **107**, 281–292 (1995)
18. Heathcote, A., Brown, S., Mewhort, D. The power law repealed: The case for an exponential law of practice. Psychol Bull **7**(2), 185–207 (2000)

19. Hinton, B. Using coherence assumptions to discover the underlying causes of the sensory input. In: Connectionism: Theory and Practice (Vancouver Series in Cognitive Science) (1992). (Paperback – Aug 20, 1992)
20. Jiang, Y., Saxe, R., Kanwisher, N. Functional magnetic resonance imaging provides new constraints on theories of the psychological refractory period. Psychol Sci **15**(6), 390–396 (2004)
21. John, B. Typist: A theory of performance in skilled typing. Hum Comput Interact **11**, 321–355 (1996)
22. John, B. Contributions to engineering models of human-computer interaction. Ph.D. Thesis, Department of Psychology, Carnegie-Mellon University (1988)
23. Jueptner, M., Weiller, C. A review of differences between basal ganglia and cerebellar control of movements as revealed by functional imaging studies. Brain **121**, 1437–1449 (1998)
24. Laird, J., Newell, A., Rosenbloom, P. Soar: An architecture for general intelligence. Artif Intell **33**, 1–64 (1987)
25. Levy, J., Pashler, H., Boer, E. Central interference in driving – is there any stopping the psychological refractory period? Psychol Sci **17**(3), 228–235 (2006)
26. Liu, Y. Queuing network modeling of elementary mental processes. Psychol Rev **103**, 116–136 (1996)
27. Liu, Y. Queuing network modeling of human performance of concurrent spatial and verbal tasks. IEEE Trans Syst, Man, Cybern **27**, 195–207 (1997)
28. Liu, Y., Feyen, R., Tsimhoni, O. Queuing network-model human processor (QN-MHP):A computational architecture for multi-task performance in humanmachine systems. ACM Trans Comput-Hum Interact **13**(1), 37–70 (2006)
29. Luck, S. An Introduction to the Event-Related Potential Technique, The MIT Press, Boston, MA (2005)
30. McCloskey, M. Networks and theories – the place of connectionism in cognitive science. Psychol Sci **2**(6), 387–395 (1991)
31. Meyer, D., Kieras, D. A computational theory of executive cognitive processes and multiple-task performance.1. basic mechanisms. Psychol Rev **104**(1), 3–65 (1997)
32. Mitz, A., Godschalk, M., Wise, S. Learning-dependent neuronal-activity in the premotor cortex – activity during the acquisition of conditional motor associations. J Neurosci **11**(6), 1855–1872 (1991)
33. Nakahara, H., Doya, K., Hikosaka, O. Parallel cortico-basal ganglia mechanisms for acquisition and execution of visuomotor sequences. J Cogn Neurosci **13**(5), 626–647 (2001)
34. Pashler, H. Processing stages in overlapping tasks – evidence for a central bottleneck. J Exp Psychol-Hum Percept Perform **10**(3), 358–3 (1984)
35. Rektor, I., Kanovsky, P., Bares, M. A SEEG study of ERP in motor and premotor cortices and in the basal ganglia. Clin Neurophysiol **114**, 463–471 (2003)
36. Roland, P. Brain Activation. John Wiley &Sons, New York (1993)
37. Romero, D., Lacourse, M., Lawrence, K. Event-related potentials as a function of movement parameter variations during motor imagery and isometric action. Behav Brain Res **117**, 83–96 (2000)
38. Rudell, A., Hu, B. Does a warning signal accelerate the processing of sensory information? evidence from recognition potential responses to high and low frequency words. Int J Psychophysiol **41**, 31–42 (2001)
39. Rumelhart, D., McClelland, J. Parallel Distributed Processing: Explorations in the Microstructure of Cognition. MIT Press, Cambridge, MA (1986)
40. Sakai, K., Hikosaka, O., Miyauchi, S., Takino, R., Sasaki, Y., Putz, B. Transition of brain activation from frontal to parietal areas in visuomotor sequence learning. J Neurosci **18**(5), 1827–1840 (1998)
41. Salthouse, T. Effects of age and skill in typing. J Exp Psychol: General **113**, 345–371 (1984)
42. Salthouse, T. Perceptual, cognitive, and motoric aspects of transcription typing. Psychol Bull **99**(3), 303–319 (1986)
43. Salthouse, T., Saults, J. Multiple spans in transcription typing. J Appl Psychol **72**(2), 187–196 (1987)

44. Selst, M.V., Ruthruff, E., Johnston, J. Can practice eliminate the psychological refractory period effect? J Exp Psychol: Hum Percept Perform **25**(5), 1268–1283 (1999)
45. Sutton, R., Barto, A. Reinforcement Learning: An Introduction. MIT Press, Cambridge, MA (1998)
46. Tsimhoni, O., Liu, Y. Modeling steering with the queuing network-model human processor (QN-MHP). In: Proceedings of the 47th Annual Conference of the Human Factors and Ergonomics Society, pp. 81–85 (2003)
47. Wu, C., Liu, Y. Modeling behavioral and brain imaging phenomena in transcription typingwith queuing networks and reinforcement learning algorithms. In: Proceedings of the 6th International Conference on Cognitive Modeling (ICCM-2004), pp. 314–319. Pittsburgh, PA (2004)
48. Wu, C., Liu, Y. Modeling human transcription typing with queuing networkmodel human processor. In: Proceedings of the 48th Annual Meeting of Human Factors and Ergonomics Society. New Orleans, Louisiana (2004). In press AQ14
49. Wu, C., Liu, Y. Modeling psychological refractory period (PRP) and practice effect on 41 PRP with queueing networks and reinforcement learning algorithms. In: Proceedings of the 6th International Conference on Cognitive Modeling (ICCM-2004), pp. 320–325. Pittsburgh, PA (2004)
50. Wu, C., Liu, Y. Modeling psychological refractory period (PRP) and practice effect on PRP with queuing networks and reinforcement learning algorithms. In: Proceedings of the Sixth International Conference on Cognitive Modeling. Pittsburgh, PA (2004). In press AQ15
51. Wu, C., Liu, Y. Modeling fMRI bold signal and reaction time of a dual task with a 42 queuing network modeling approach. In: 28th Annual Conference of the Cognitive Science Society. Vancouver, BC, Canada (2006)
52. Wu, C., Liu, Y. Queuing network modeling of a real-time psychophysiological index of mental workload.p300 amplitude in event-related potential (ERP). In: Paper presented at the 50th Annual Conference of the Human Factors and Ergonomics Society. San Francisco, CA (2006)
53. Wu, C., Liu, Y. Queuing network modeling of age differences in driver mental workload and performance. In: 50th Annual Conference of the Human Factors and Ergonomics Society. San Francisco, CA (2006)
54. Wu, C., Liu, Y. Queuing network modeling of driver workload and performance. In: 50th Annual Conference of the Human Factors and Ergonomics Society. San Francisco, CA (2006)
55. Wu, C., Liu, Y. Queuing network modeling of reaction time, response accuracy, and stimulus-lateralized readiness potential onset time in a dual task. In: 28th Annual Conference of the Cognitive Science Society. Vancouver, BC, Canada (2006)
56. Wu, C., Liu, Y. A new software tool for modeling human performance and mental workload. Q Hum Factors Appl: Ergon Des **15**(2), 8–14 (2007)
57. Wu, C., Liu, Y. Queueing network modeling of transcription typing. ACM Trans Comput-Hum Interact (2007). In Press AQ16
58. Wu, C., Liu, Y. Queuing network modeling of driver workload and performance. IEEE Trans Intell Transport Syst **8**(3), 528–537 (2007)
59. Wu, C., Liu, Y., Tsimhoni, O. Application of schedulingmethods in designing multimodal in-vehicle systems. In: Society of Automobile Engineers (SAE) World Congress. SAE, Detroit, MI (2008)
60. Wu, C., Liu, Y., Walsh, C. Queuing network modeling of a real-time psychophysiological index of mental workload–p300 in event-related potential (ERP). IEEE Trans Syst, Man, Cybern (Part A) (2007). In press AQ17
61. Wu, C., Tsimhoni, O., Liu, Y. Development of an adaptive workload management system using queuing network-model of human processor. In: The 51st Annual Conference of the Human Factors and Ergonomics Society. Baltimore, MD (2007) AQ18
62.